2nd EUJAPAN DIGITAL WEEK 2026

Tailoring the Physical Properties of Narrow-Gap Semiconductor Mg_2Sn Thermoelectric Thin Films through Defect Engineering

Takeaki Sakurai[1], Takao Mori[2]

[1]University of Tsukuba

[2]National Institute for Materials Science

Thermoelectric Materials

Attracting increasing attention because they can directly convert WASTE heat to electricity via Seebeck effect

Three basic thermoelectric effects that explains the behavior of direct conversion between electricity and temperature gradient

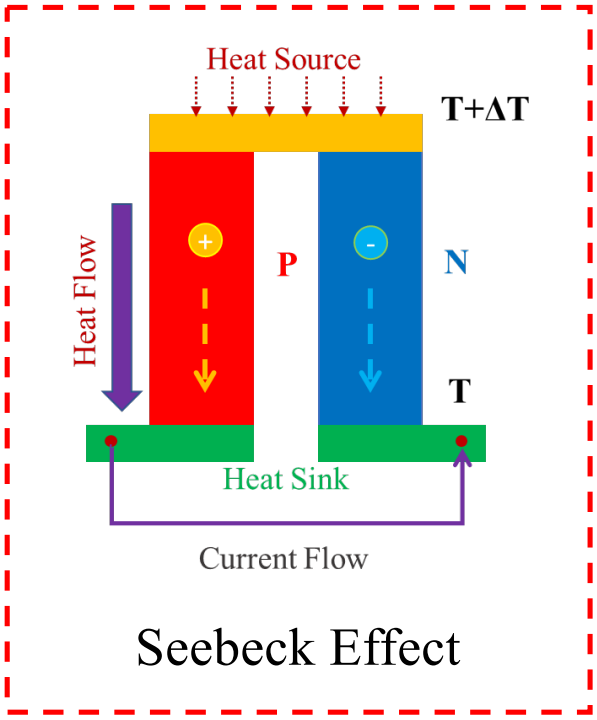

Seebeck Effect

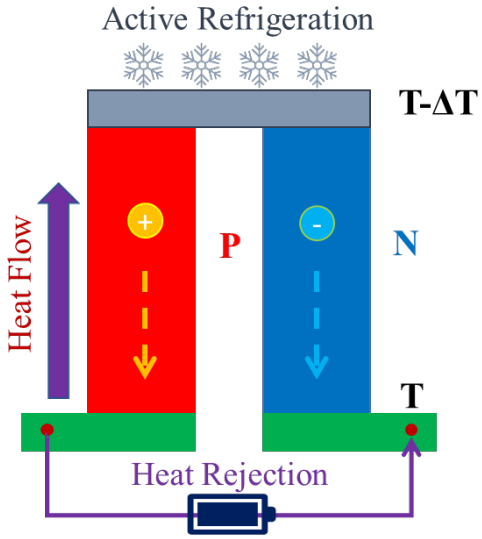

Peltier Effect

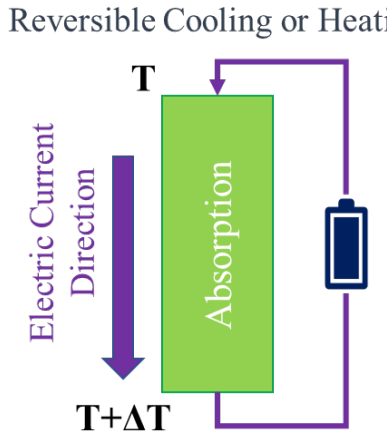

Thomson Effect

Thermoelectric- Figure of Merit (ZT)

Thermoelectric device Efficiency

$$\eta = \left(\frac{T_{hot} - T_{cold}}{T_{hot}}\right)\left[\frac{\sqrt{1+ZT_m} - 1}{\sqrt{1+ZT_m} + \left(\frac{T_{cold}}{T_{hot}}\right)}\right]$$

$$ZT = \frac{S^2\sigma T}{\kappa} = \frac{PF}{\kappa}T \qquad T_m = \frac{T_{hot} - T_{cold}}{2}$$

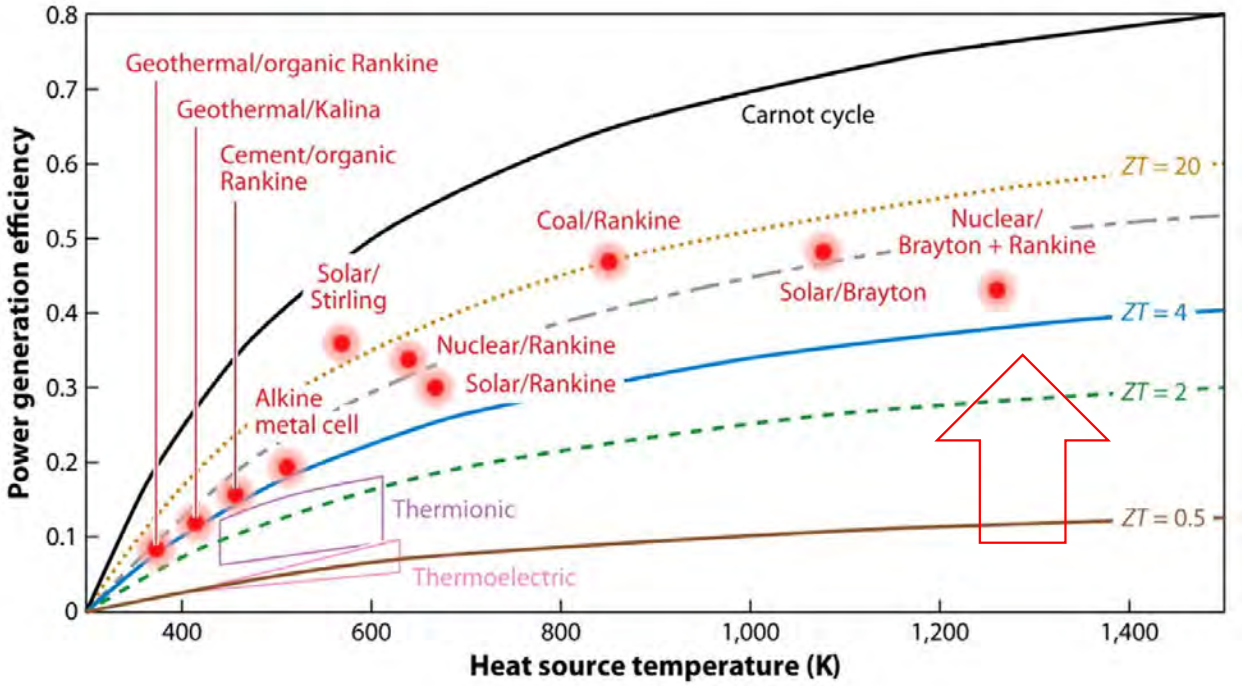

ZT : Figure of Merit
S : Seebeck coefficient
σ : electrical conductivity
κ : thermal conductivity
T : Temperature
PF: Power Factor

For thin film devices applications :

PF = $S^2\sigma$ ⇨ Power output

He et al., Science 357, eaak9997 (2017)

Thermoelectric Materials Applications

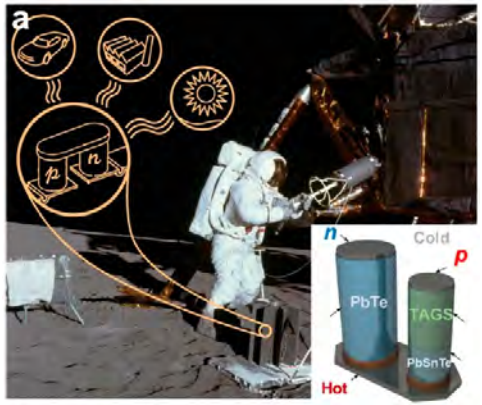

Space Applications

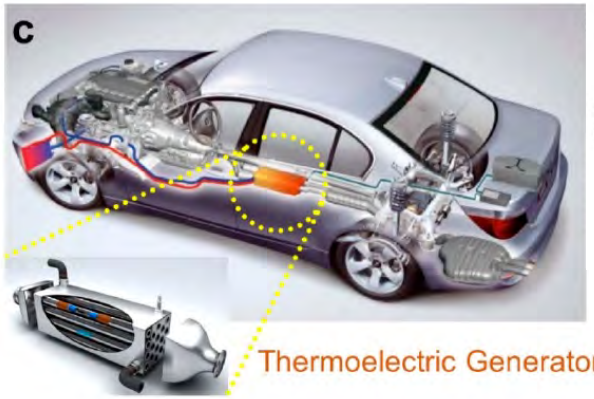

Automobile Applications

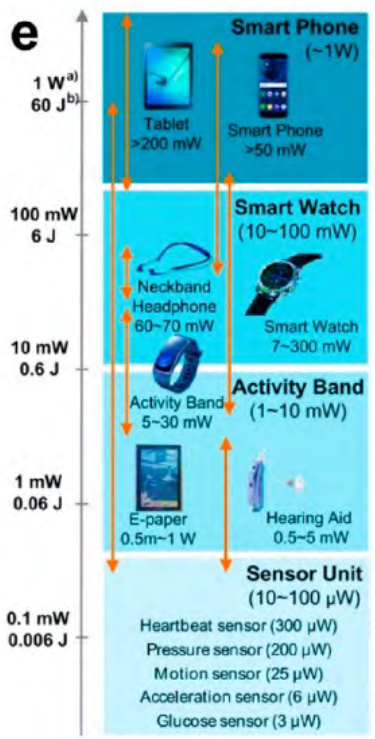

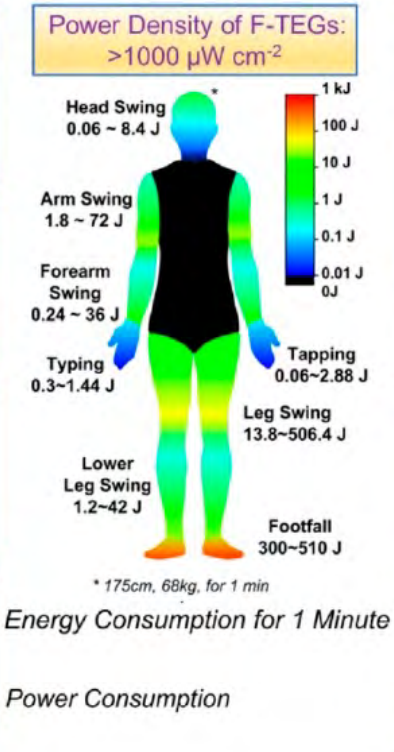

https://dx.doi.org/10.1021/acs.chemrev.0c00026

Wearable Electronics Applications

Thermoelectric Thin Films

- ✓ Suitable for miniaturized TE devices (compared to bulk counterparts)
- ✓ Applicability in microdevices for IoT applications
- ✓ Potential for high power density

High-Performing Thin Films

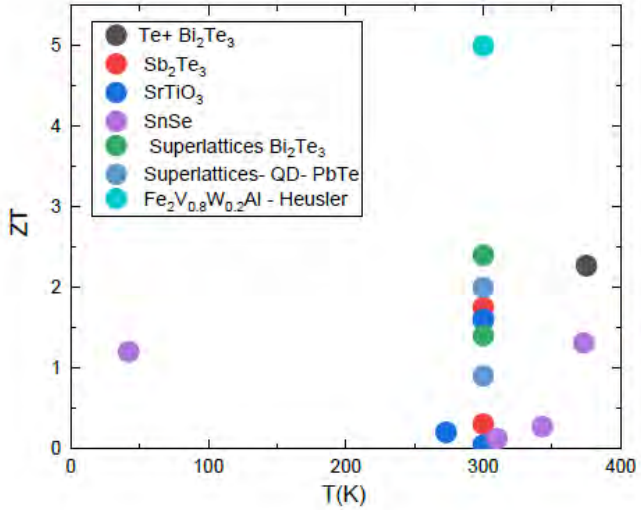

Drawbacks

$ or

Thin films Target

Low-cost material and Environment-friendly

Thin film Mg- based

Why Mg-based thermoelectric film?

Advantages

- Environment-friendly
- Cubic structure
- Narrow gap
- High n-type performance

Issues of Mg-based

- Low p-type performance
- High thermal conductivity

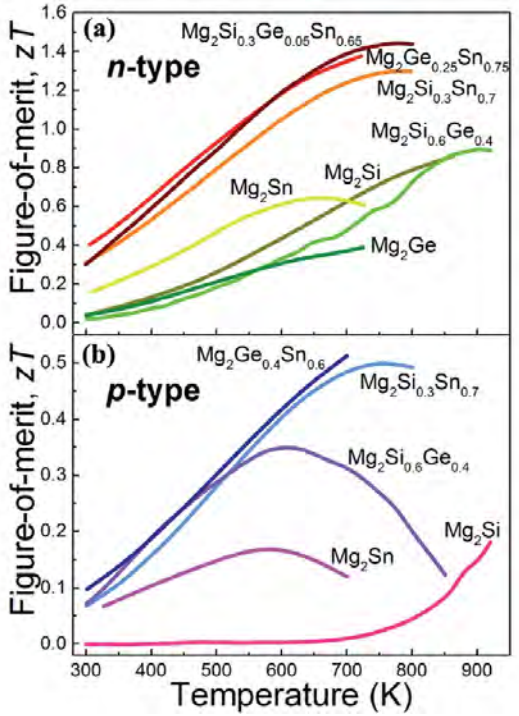

R. Venkatasubramanian,. Nature 413, 597–602 (2001).
T.Harman at el., Science 297, ,2229–2232, (2002)
B. Hinterleitner at el, *Nature* **576,** 85–90 (2019)
G. Jeffrey Snyder Energy Harvesting Technologies (Springer 2008)

Engineering TE Materials

- $S^2\sigma$
  - Carrier Concentration
  - Valence Control

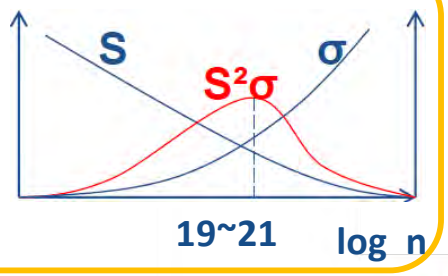

Goal: secure a high ZT

$$zT = \frac{S^2\sigma}{\kappa}T = \frac{S^2\sigma}{\kappa_e+\kappa_l}T$$

- S/κ
  - DOS control
  - $DOS(E)=m^*/\pi h d_w$, d_w: quantum well

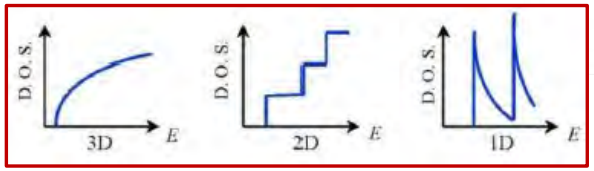

Coupling

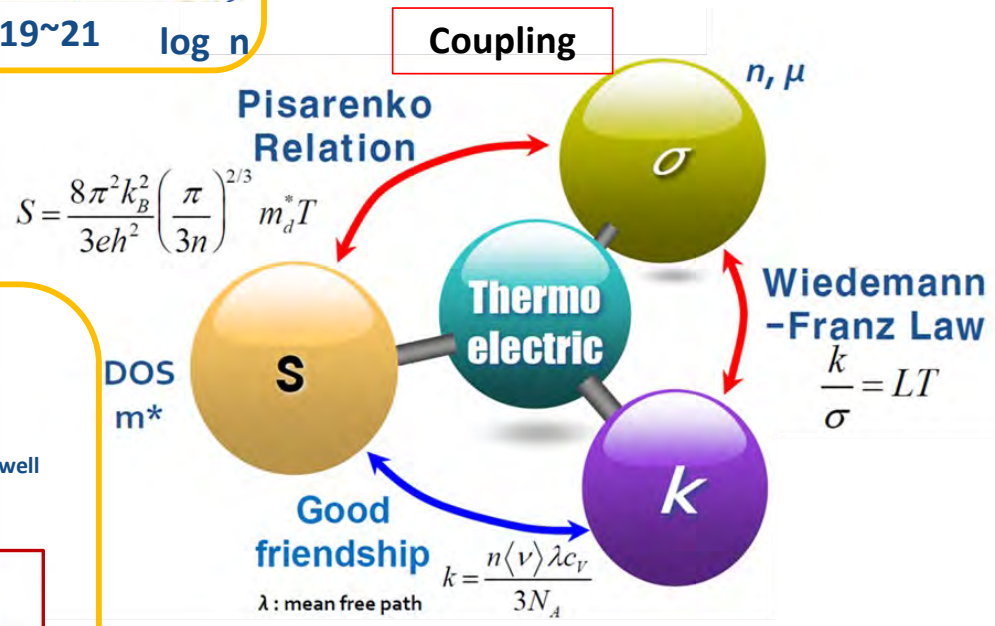

Decoupling

- σ/κ
  - Defects Engineering

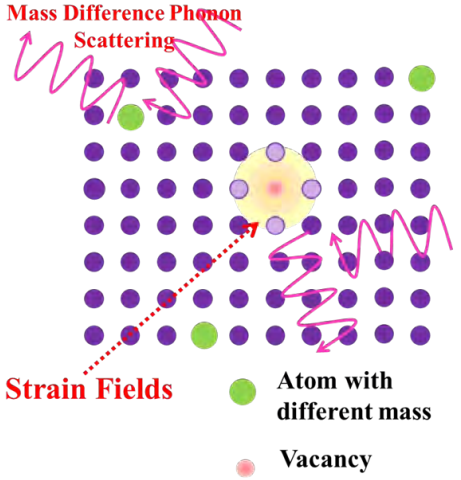

Thermal conduct

$$ZT = \frac{\alpha^2 \sigma T}{\kappa} = \frac{PF}{\kappa_{el} + \kappa_{latt}} T$$

$$\kappa_{latt} = \left(\frac{k_B}{2\pi^2 v}\right)\left(\frac{k_B T}{\hbar}\right)\int_0^{\theta_D/T} \frac{x^4}{\tau_{total}^{-1}\,(e^{-x}-1)^2}\,dx\,,x \equiv \frac{\hbar\omega}{k_B T}$$

$$\tau_{total}^{-1} = \tau_U^{-1} + \tau_d^{-1} + \tau_{pd}^{-1}$$

τ_U^{-1} = Umklapp processes

τ_d^{-1} = Dislocations $\Rightarrow$ $\tau_{pd}^{-1} = \frac{V^{4/3}\omega^3}{v^2} N_{DC}$,

τ_{pd}^{-1} = Point Defects $\Rightarrow$ $\tau_{pd}^{-1} = \frac{V\omega^4}{4\pi v^4}\Gamma$, $\quad \Gamma \sim \left(\frac{\Delta M}{M}\right)^2$

Γ = Disorder parameter $\quad N_D$ = Dislocation density

v = average sound velocity $\quad \theta_D$ = Debye temperature

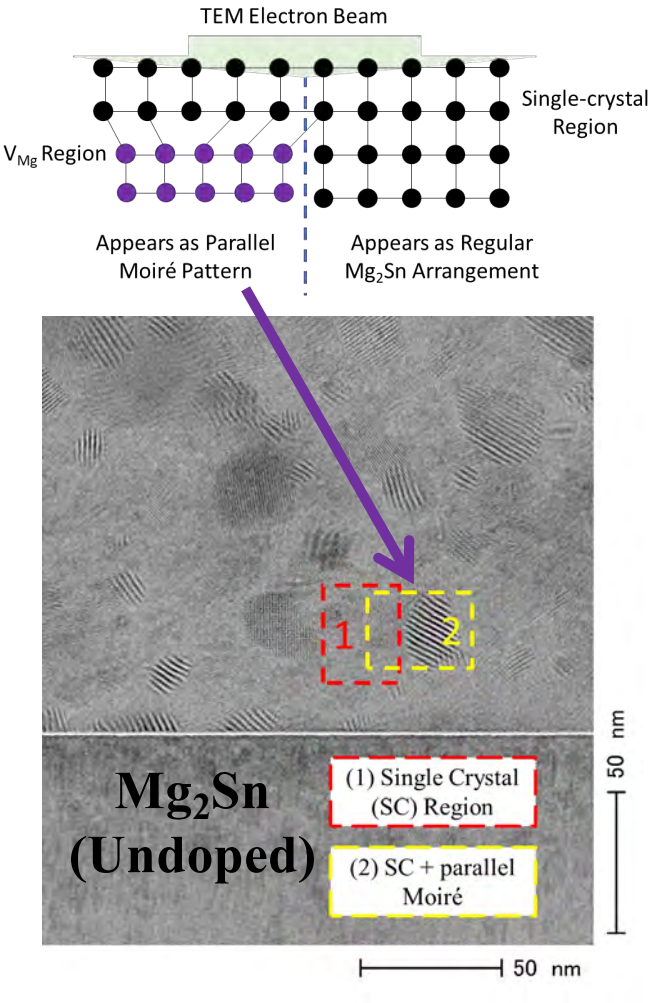

1 Ge alloying and point defects engineering – Why Ge?

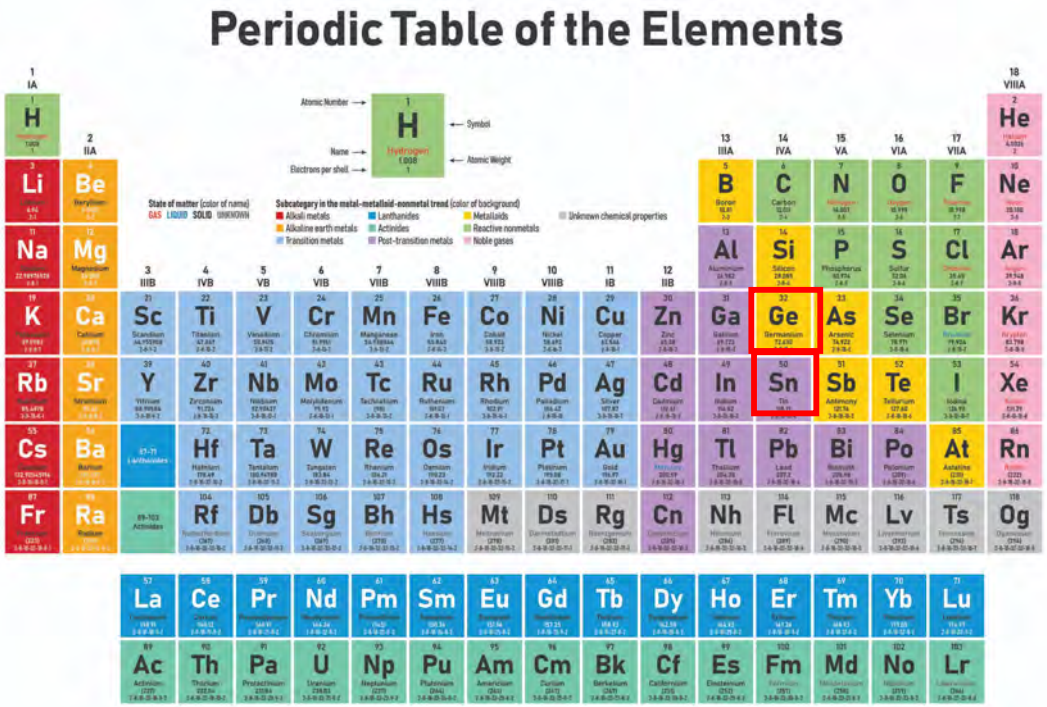

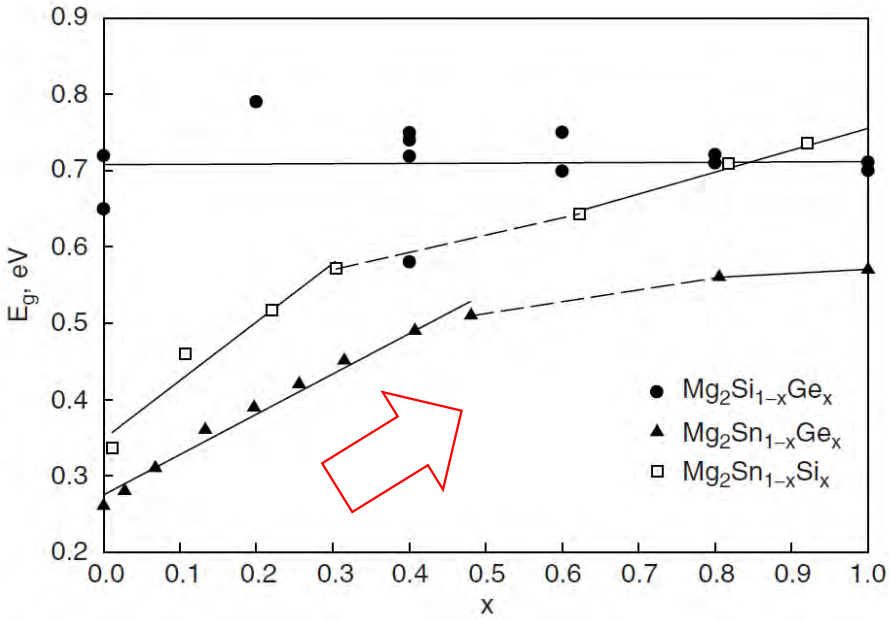

- Ge increase the band gap of the material which could reduce the bipolar effect.
- Difference in the mass between Ge and Sn, phonon scatting center.

Ge incorporation – Thermoelectric Properties

Mariana S. L. Lima *et al* 2021 *Jpn. J. Appl. Phys.* **60** SBBF06

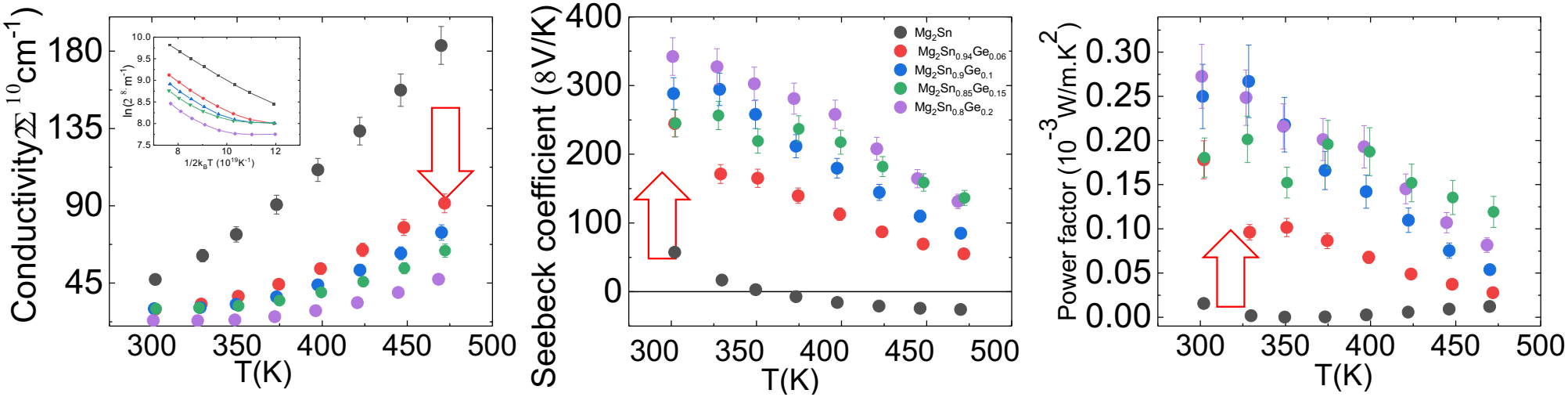

- The conductivity systematic reduce with the incorporation Ge, suggesting an increase in the band gap in the material.
- The Seebeck coefficient improve p-type improve with strong dependence on temperature, suggesting the bipolar effect transition was shifted to higher temperature.
- The p-type behavior suggest the intrinsic point defect inside of our material are Mg vacancies (V_{Mg}).

Ge incorporation- $Mg_2Sn_{1-x}Ge_x$

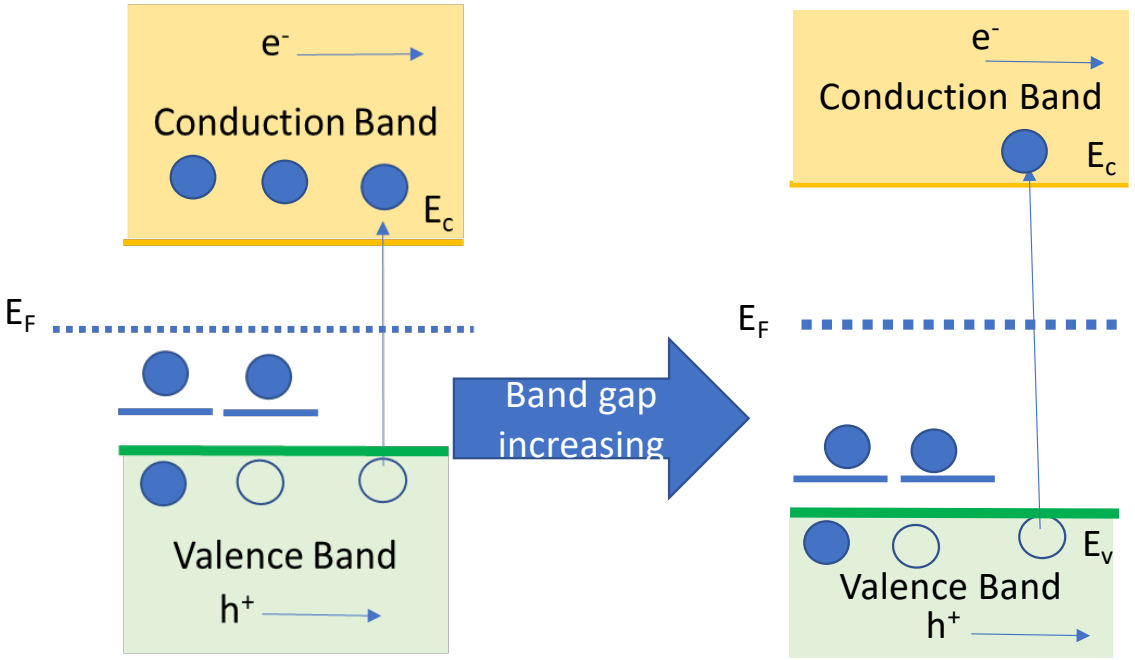

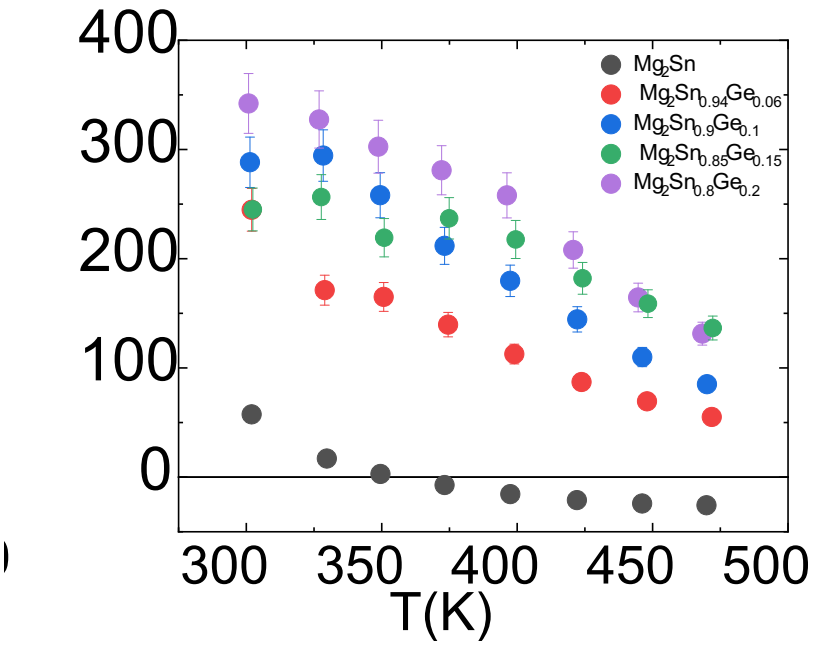

- From XRD and conductivity data, the band gap increase with Ge incorporation.
- In case of Mg_2Sn, the bipolar peak occurs at low temperature. At room temperature, the difference between majority and minority was reduce. So, the total Seebeck coefficient is very small.
- In case of $Mg_2Sn_{1-x}Ge_x$, the bipolar peak probably occurred at around room temperature. So, the minority carrier increase the conductivity, but reduce the Seebeck coefficient.

+ Generation of Mg vacancy (Increase in density of acceptor level)

Defects in Thermoelectric Materials

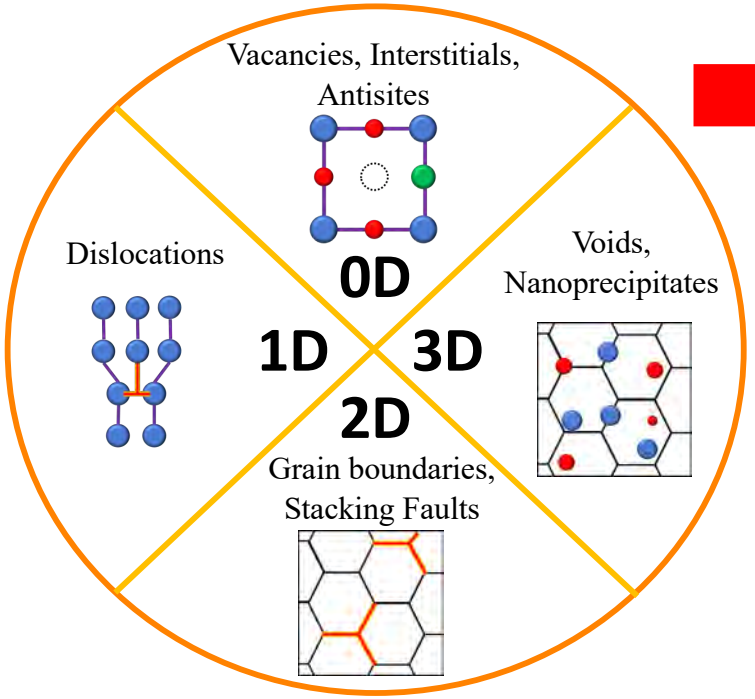

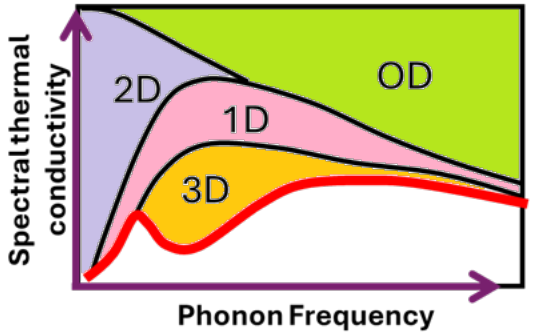

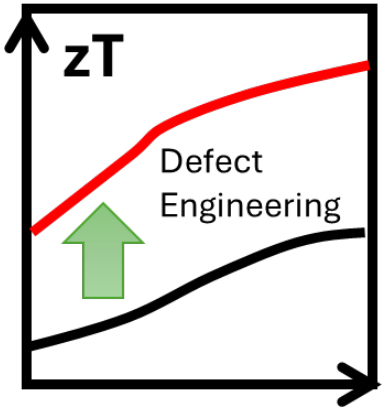

$$ZT = \frac{\alpha^2 \sigma T}{\kappa} = \frac{PF}{\kappa_{el} + \kappa_{latt}} T$$

$$\kappa_{latt} = \left(\frac{k_B}{2\pi^2 v}\right)\left(\frac{k_B T}{\hbar}\right)\int_0^{\theta_D/T} \frac{x^4}{\tau_{total}^{-1}\,(e^{-x}-1)^2}\,dx\,,x \equiv \frac{\hbar\omega}{k_B T}$$

$$\tau_{total}^{-1} = \tau_U^{-1} + \tau_d^{-1} + \tau_{pd}^{-1} + \tau_{sf}^{-1} + \ldots +$$

How to observe?

0D: Electron/neutron scattering, synchrotron XRD, **Positron Annihilation Spectroscopy**

1D: TEM, Syn-PXRD + modified Williamson-hall model

Mg-vacancy in $Mg_2Sn_{1-x}Ge_x$ Films

Positron Annihilation Results

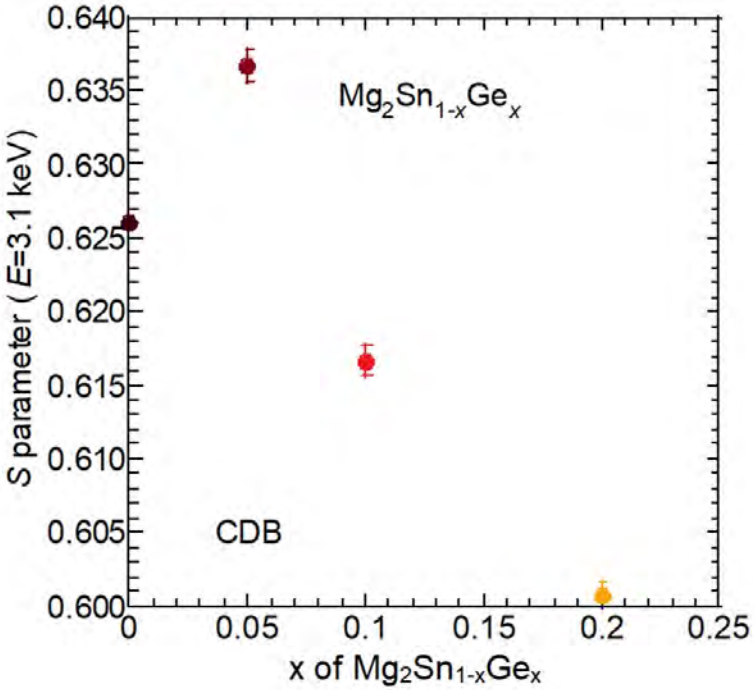

Increase in S parameter

↓

Increase in defect concentration

K.M. Senados *et al* 2024 *Jpn. J. Appl. Phys.* **63** 02SP40

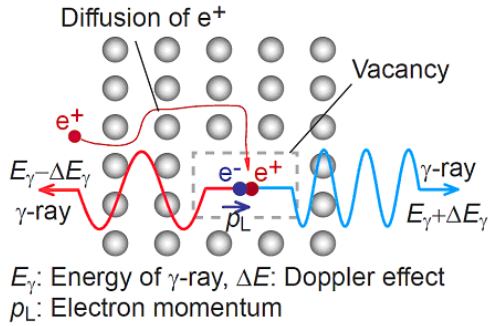

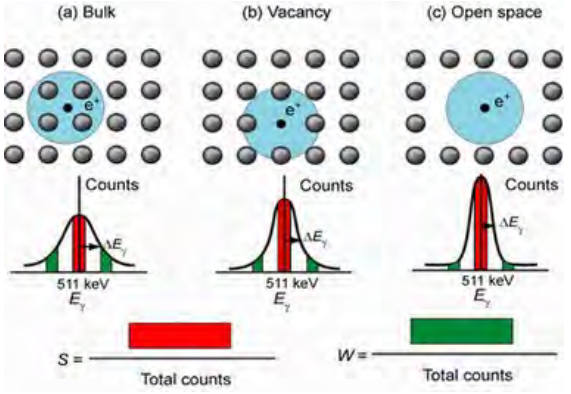

- Vacancy-type defects can be detected by measuring the energy distribution of annihilation gamma rays (S parameter)

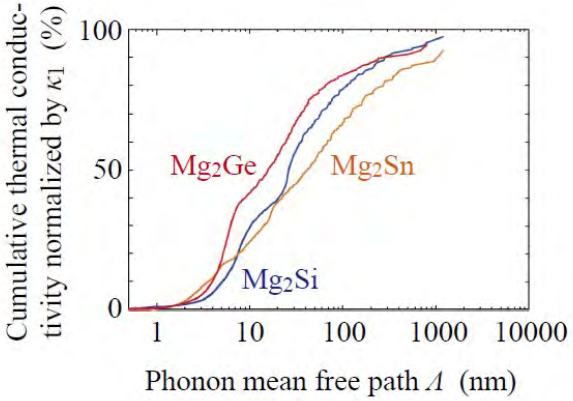

Increase defect concentration → average distance between point defects are shortened → significant decrease in κ is observed

D. Aketo, T. Shiga, and J. Shiomi, Appl. Phys. Lett. 105, 131901 (2014).

Thermal Conductivity at RT of $Mg_2Sn_{1-x}Ge_x$ Films with Point Defects

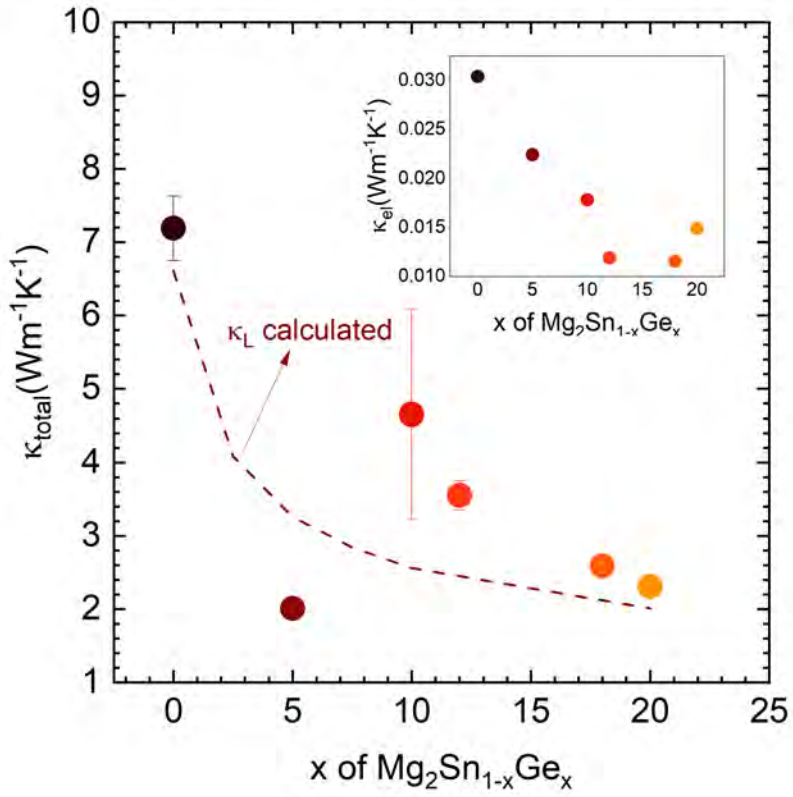

Wiedemann-Franz law

$$\kappa_{el} = L\sigma T, \qquad L = 1.5 + \exp\left(-\frac{|S|}{116}\right)$$

Bipolar conduction

$$\kappa_{bip} = \frac{\sigma_n \sigma_p}{\sigma_n + \sigma_p}\left(\alpha_n - \alpha_p\right)^2 T$$

suppressed with Ge incorporation (robust p-type behavior)

Debye model

$$\kappa_{latt} = \left(\frac{k_B}{2\pi^2 v}\right)\left(\frac{k_B T}{\hbar}\right)\int_0^{\theta_D/T} \frac{x^4 e^x}{\tau_{total}^{-1}\,(e^{-x}-1)^2}\,dx\,, x \equiv \frac{\hbar\omega}{k_B T}$$

$$\tau_{total}^{-1} = \tau_U^{-1} + \tau_d^{-1} + \tau_{pd}^{-1}$$

$$\tau_{pd}^{-1} = \frac{V\omega^4}{4\pi v^4}\,\Gamma\,, \qquad \Gamma \sim \left(\frac{\Delta M}{M}\right)^2 \qquad \tau_d^{-1} \propto N_D \frac{r^4}{v^2}\omega^3$$

κ_L (Umklapp process) was approximated using d3q code of QUANTUM ESPRESSO

Ge alloying of epitaxial Mg_2Sn films is an effective strategy to lower thermal conductivity due to additional phonon scattering provided by mass difference, point defects and dislocations.

2 Defects Modification – Mg flux rate

K.M. Senados *et al* 2025 *J. Physics Energy* ***7*** *035001*

Positron Annihilation Spectroscopy (PAS)

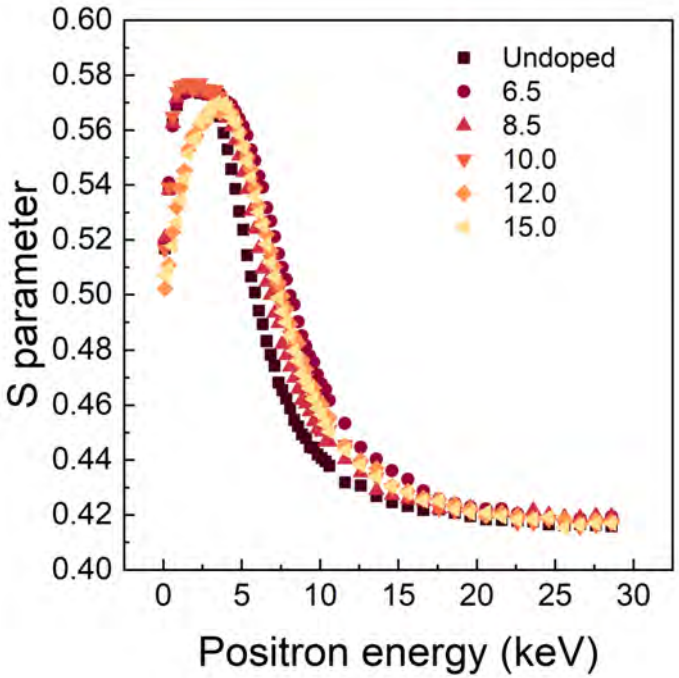

reduction of vacancy-type defects
(decrease in S parameter)

X-Ray Rocking Curve

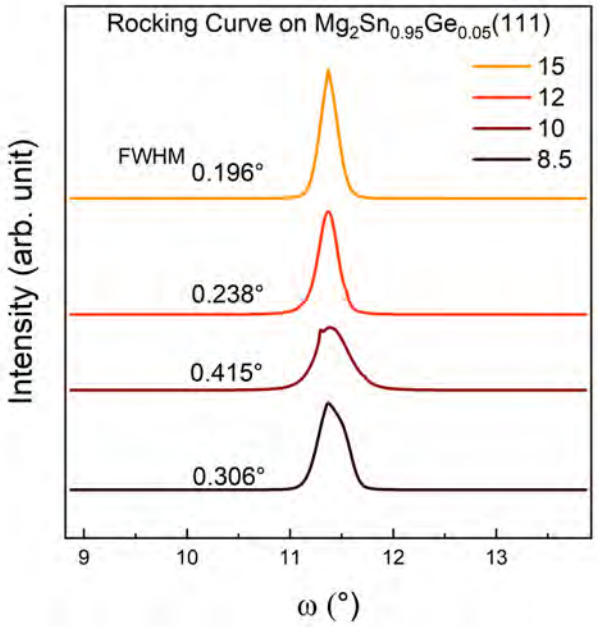

higher crystallinity at
higher Mg flux rates

Representative Pole Figure
$Mg_2Sn_{0.95}Ge_{0.05}$\{220\}

Mg Flux Rate
~8.0 $atoms \cdot s^{-1}nm^{-2}$

Mg Flux Rate
~15.0 $atoms \cdot s^{-1}nm^{-2}$

Stacking faults (pointed in →)
form at higher flux rates

- Excess Mg, has high vapor pressure, predominantly desorb during film growth
- Modulation of Mg flux plays a significant role in quality and concentration of defects

Thermal Conductivity at RT of $Mg_2Sn_{1-x}Ge_x$ Films as Mg flux rate changes

K.M. Senados *et al* 2025 *J. Physics Energy* ***7*** *035001*

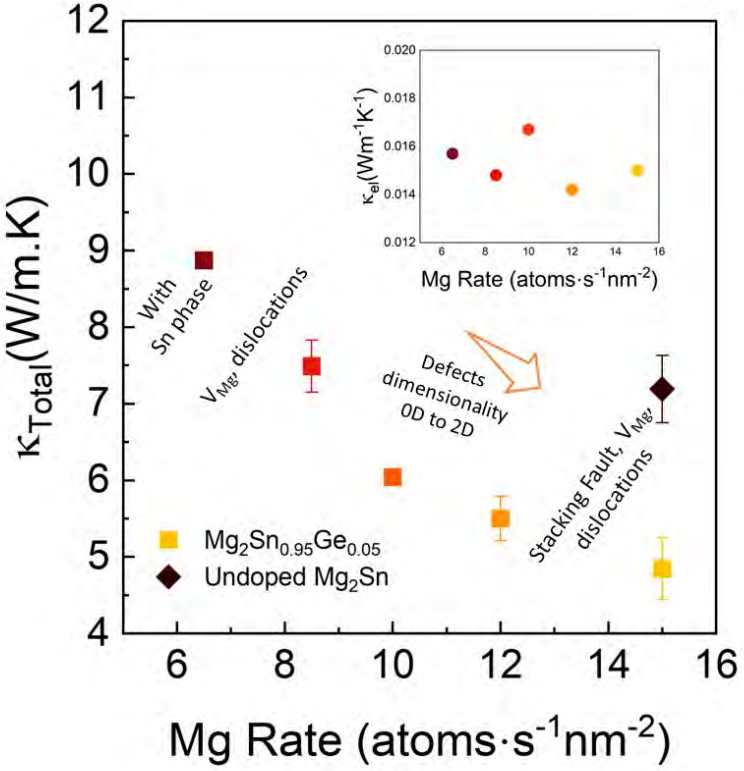

By modulating Mg flux rates in MBE-grown Mg_2Sn thin films, it is possible to achieve enhanced crystalline alignment and controlled formation of beneficial higher-dimensionality defects, which together contribute to the reduction in thermal conductivity.

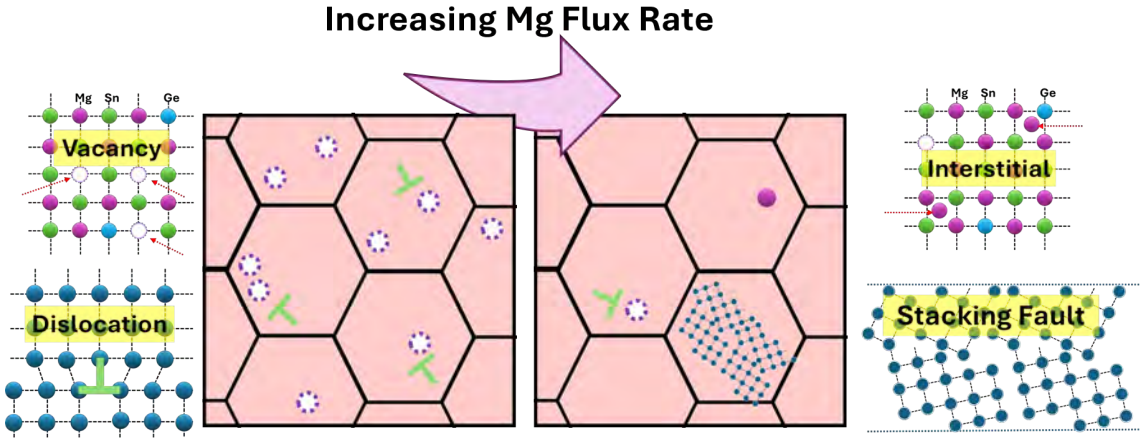

$$\tau_C^{-1} = \tau_U^{-1} + \tau_N^{-1} + \tau_{PD}^{-1} + \tau_{DC}^{-1} + \tau_B^{-1} + \tau_{SF}^{-1} \ldots$$

Additional scattering processes from higher dimensionality defects

3 Improvement of p-Mg_2Sn film by Doping – Ga? Li?

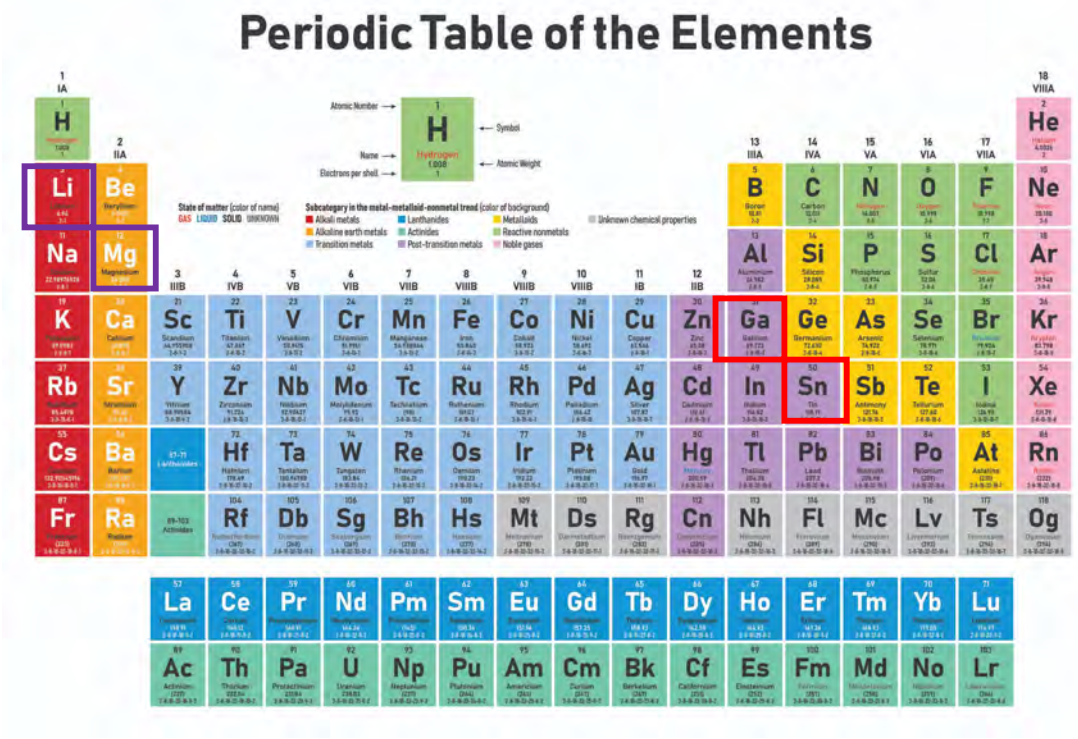

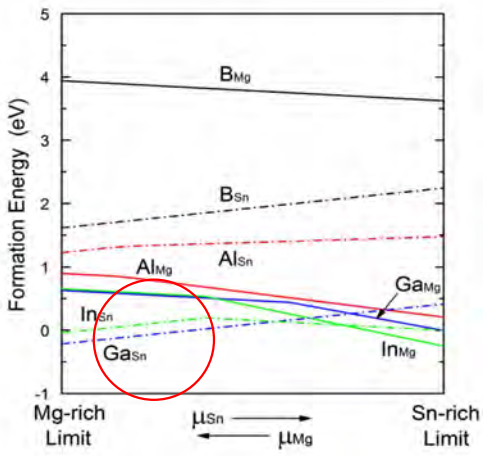

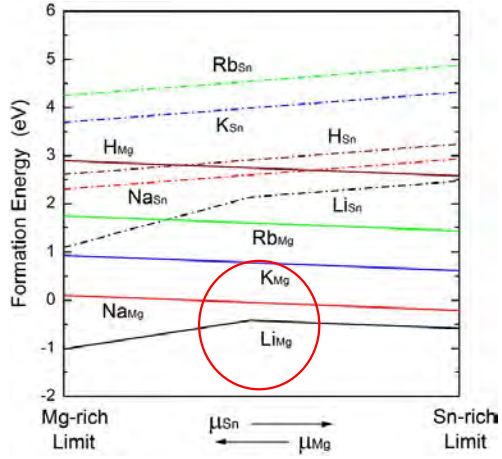

J. Tani, H. Kido / Physica B 407 (2012) 3493–3498

- Ga_{Sn} and/or Li_{Mg} both has low formation energy.
- p-type doping in Sn (for Ga) and Mg (for Li) sites.
- The ionic radius is closed to Sn, Mg which will keep epitaxial nature.
- Difference in the mass between host atom (Sn, Mg) and dopant (Ga, Li)phonon scatting center

Ga doping – Thermoelectric Properties

Mariana S. L. Lima *et al* 2021 *Appl. Phys. Lett.* **119** 254101

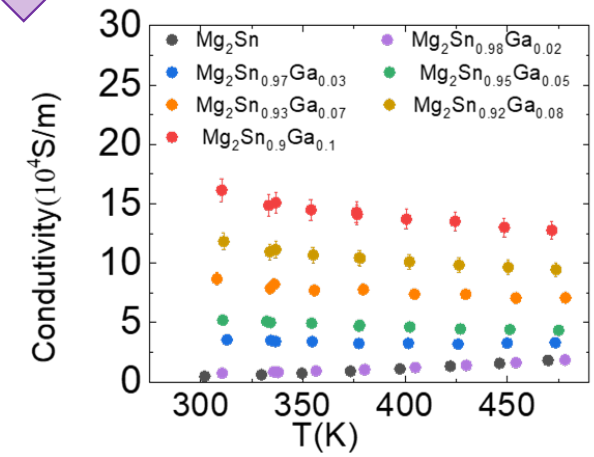

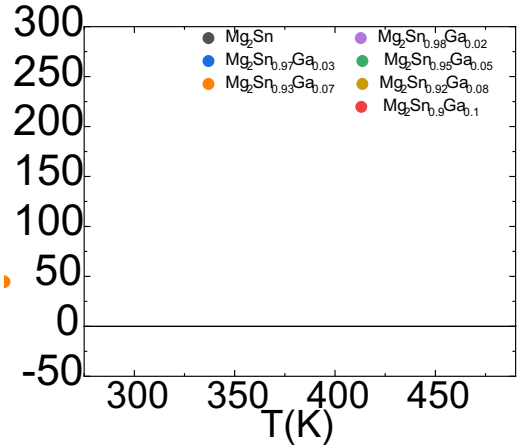

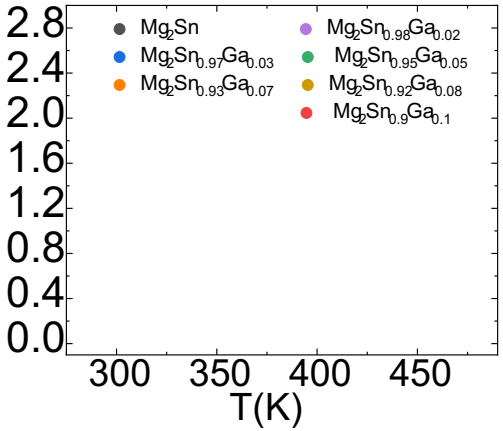

- T
- C

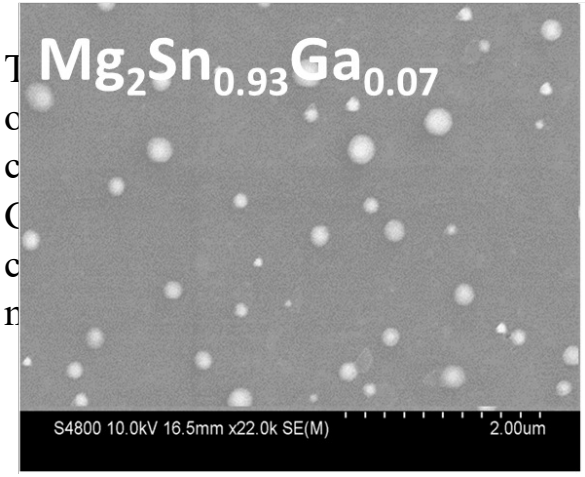

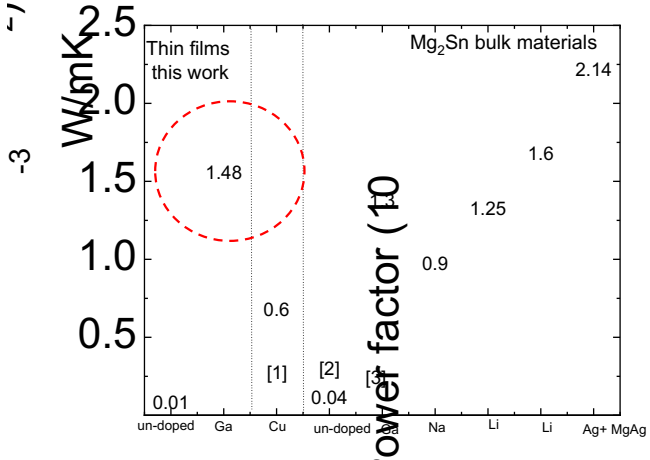

The combination of the shift in the conductivity and Seebeck coefficient result in high power factor for light doped samples. The improvement was around 100 times with the Ga incorporation.

[1] Safavi et al. J. Electron. Mater. volume 50, pages 2738–2749 (2021)
[2]Z. Huang et al. ACS Appl. Energy Mater. 2021, 4, 13044−13050 (2021)
[3:Li, X., Li, S., Feng, S. & Zhong, H. Intermetallics 81, 26–31 (2017)
[4]Jichi Tani,, Shinagawa, T. & Chigane, M. J. Electron. Mater. 48, 3330–3335 (2019).
[5]H. Kamila, et al..J. Mater. Chem. A 7, 1045–1054 (2019) supplementary material
[6]H. Y, Chen, et al. Phys. Status Solidi Appl. Mater. Sci. 207, 2523–2531 (2010).

*Li-doped Mg_2Sn

Under review

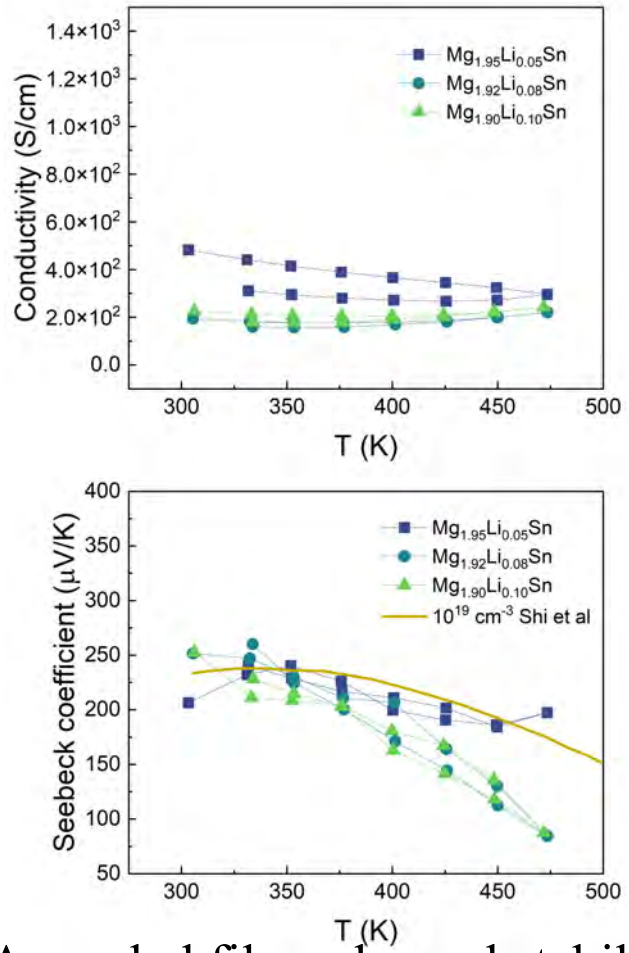

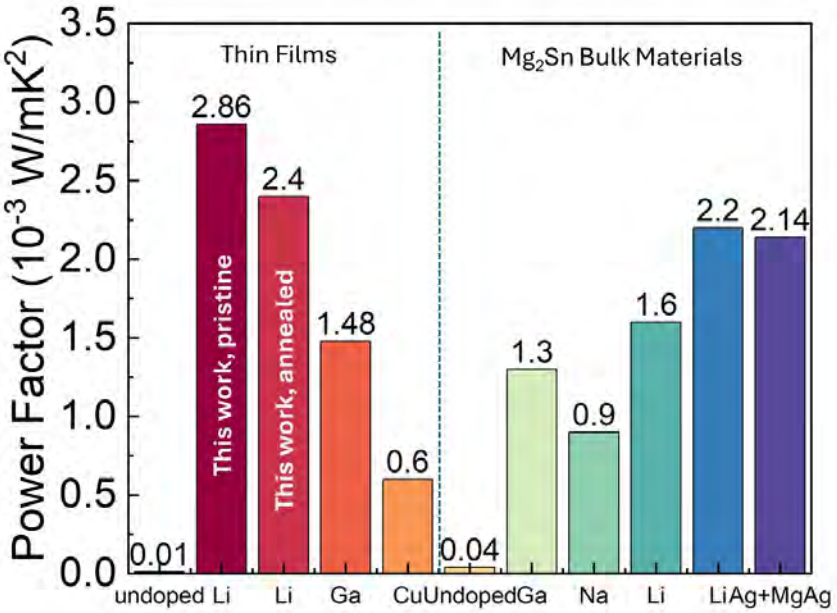

[1] Lima et al., Appl. Phys. Lett, 119, 254101 (2021)
[2] Safavi et al. J. Electron. Mater. volume 50, pages 2738–2749 (2021)
[3]Z. Huang et al. ACS Appl. Energy Mater. 2021, 4, 13044−13050 (2021)
[4:Li, X., Li, S., Feng, S. & Zhong, H. Intermetallics 81, 26–31 (2017)

[5]Jichi Tani,, Shinagawa, T. & Chigane, M. J. Electron. Mater. 48, 3330–3335 (2019).
[6]H. Kamila, et al..J. Mater. Chem. A 7, 1045–1054 (2019) supplementary material
[7] Z. Huang et al., J. Mater. Chem. A 11, 2652-2660 (2023(
[8]H. Y, Chen, et al. Phys. Status Solidi Appl. Mater. Sci. 207, 2523–2531 (2010).

- Highest PF ~ 2.86×10^{-3} (As-grown at 450 K), PF ~2.40×10^{-3} (Annealed 350K)

Annealed films showed stability and improved p-type properties, improved Seebeck near room temperature

Acknowledgement

This work is partially supported by JST-MIRAI.

Thank you for your attention